Behavior of hydrogen isotope retention in carbon implanted tungsten

Yasuhisa Oya [a,*], Yuji Inagaki [a], Sachiko Suzuki [a], Hirotada Ishikawa [a], Yohei Kikuchi [a], Akira Yoshikawa [a], Hirotomo Iwakiri [b], Naoko Ashikawa [c], Akio Sagara [c], Naoaki Yoshida [b], Kenji Okuno [a]

[a] Radioscience Research Laboratory, Faculty of Science, Shizuoka University, 836, Ohya, Suruga-ku, Shizuoka 422-8529, Japan
[b] Institute of Applied Mechanics, Kyushu University, Japan
[c] National Institute for Fusion Science, Japan

ARTICLE INFO

ABSTRACT

To elucidate the C^+ implantation effect on deuterium retention in tungsten, simultaneous C^+ and D_2^+ implantation was performed on tungsten. Deuterium desorption behavior for simultaneously implanted tungsten was compared with that the sequentially implanted tungsten. It was found that deuterium retention for the simultaneous case was lower than that for the sequential one, indicating that the sputtering of carbon and deuterium trapped by carbon would prevent the deuterium trapping. In addition, deuterium retention decreased with increasing C^+/D^+ ratio and deuterium trapping by carbon was not observed for high C^+/D^+ ratio. These facts indicate that the number of available traps in tungsten produced by simultaneous ion implantation would mainly control the deuterium retention in tungsten. However, for low C^+/D^+ ratios, deuterium trapping by carbon would be one of major trapping states.

© 2009 Elsevier B.V. All rights reserved.

1. Introduction

Plasma facing materials are one key boundary in maintaining high purity D–T plasma and their selections are quite important. Recently, the combination of several different materials as plasma facing materials for the first wall, divertor and baffles was deemed to be one of the best solution [1–3]. As a result, mixed materials or plasma-created materials will form on the surface of the original while simultaneously hydrogen isotopes, including tritium, will be implanted into the mixed materials.

The tungsten–carbon system is widely studied [3–9]. Many of these reports relate the formation of carbon layers or carbides with the implantation of carbon ions. Data derived from as-received virgin materials are usually used for design activities, but these data may be quite different from the actual mixed layers formed under fusion conditions. In particular, comparison of deuterium retention is clearly dependent on the conditions of carbon implantation. Deuterium retentions in tungsten and tungsten carbide indicate that carbon ion pre-implantation decreases the D recombination coefficient and consequently increases the amount of retained deuterium [6,8]. It was also shown that deuterium retentions in W–C mixed materials were much lower than expected from the assumption that the W–C mixed material consists of tungsten and graphite precipitators [5]. These reports are based on carbon pre-implanted tungsten where mixed layers have been formed

prior to deuterium implantation. However, in a fusion environment, simultaneous implantations of carbon and deuterium ions occur dynamically involving continuous deuterium and carbon recycling processes. A previous report focused on tungsten sputtering and not deuterium retention under simultaneous carbon and deuterium ion implantation [10].

These facts motivate us to investigate deuterium trapping in tungsten under simultaneous carbon and deuterium ion implantation to understand the trapping mechanisms and determine the role of carbon on deuterium retention. Therefore, an experimental simultaneous carbon and deuterium ion implantation system was developed at Shizuoka University and applied in this study.

2. Experimental

Disk-type samples with 10 mm diameter and 0.5 mm thickness were prepared from a rod of tungsten under stress-relieved conditions supplied by Allied Tungsten Co. Ltd. The samples were polished mechanically and pre-heated at 1173 K for 10 min in vacuum to remove the surface impurities and damages induced by the polishing process.

The simultaneous carbon ion (C^+) and deuterium ion (D_2^+) implantation system combined with a thermal desorption spectroscopy (TDS) system was designed and established at Shizuoka University. The sample can be easily transferred from the ion implantation chamber to the TDS chamber via a sample introduction chamber without air exposure. CO_2 was used as the C^+ source gas to exclude hydrogen impurities. The $E \times B$ mass separator was

equipped at the head of the C^+ gun and the oxygen impurity was completely evacuated by a turbo molecular pump. The C^+ and D^+ ion was implanted using different ion guns equipped in the implantation chamber and incident angles for both ion guns were 15° to the surface normal. The implantation area was set to be 4 mm × 4 mm. The C^+ acceleration energy was controlled between 0.5 and 10 keV and the maximum ion flux was 2×10^{18} C^+ m^{-2} s^{-1}, which was estimated by a faraday cup. A ceramic heater was equipped with the sample holder to heat the samples up to 1300 K.

In the present study, to elucidate the interaction mechanism of C with D in tungsten, it is important to keep the same implantation depths of C^+ with D_2^+. SRIM [11] calculation results indicated that the implantation depth of 3 keV D_2^+ was almost the same as that of 10 keV C^+; corresponding to an implantation depth of ∼11 nm. Therefore, the ion energies of C^+ and D_2^+ were set to be 10 keV and 3 keV, respectively. At first, to evaluate the implantation sequence effect, two different implantation procedures, namely sequential and simultaneous implantations, were performed. In the sequential implantation, 10 keV C^+ implantation was performed initially with a flux of 1.0×1018 C^+ m^{-2} s^{-1} up to a fluence of 1.0×1022 C^+ m^{-2}. Thereafter, 3 keV D_2^+ implantation was done with the same ion flux and fluence as the C^+ implantation.

The C^+/D^+ flux ratio was varied from 0.2 to 2 by changing the C^+ ion flux from 2.0×1017 C^+ m^{-2} s^{-1} to 2.0×1018 C^+ m^{-2} s^{-1} while maintaining the D_2^+ ion flux and fluence at 1.0×1018 D^+ m^{-2} s^{-1} and 1.0×1022 D^+ m^{-2}, respectively.

Following the ion implantations, the chemical states of W and C were evaluated by XPS (ESCA1600 system, ULVAC-PHI Inc.) using an Al Kα X-ray source (1486.6 eV) and a hemispherical electron analyzer [8,9]. The analyzed area was set to be 720 μm × 720 μm and measurement was done in the center of the implanted area. To evaluate D desorption and retention behaviors, TDS was performed at a heating rate of 0.5 K s^{-1} up to 1300 K using a quadruple mass spectrometer.

3. Results and discussion

Fig. 1 summarizes the D_2 TDS spectra for the sequentially and simultaneously implanted tungsten. The D_2 TDS spectra for pure tungsten and WC are also shown in this figure. It was found that deuterium desorption at higher temperature only occurred for the sequentially implanted tungsten. This high desorption temperature was almost the same as that for WC, indicating that the deuterium desorption trapped by carbon. In case of simultaneously implanted tungsten, the shape of the TDS spectra was similar to
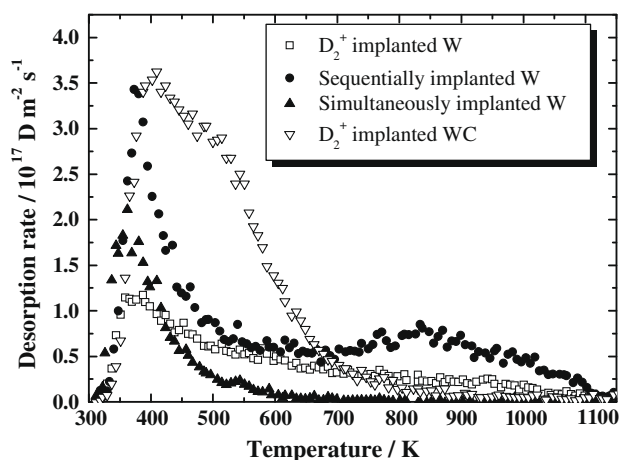
that of the pure tungsten. To evaluate the chemical state of carbon implanted into tungsten, XPS analyses were performed. Fig. 2 shows the C 1s XPS spectra for the C^+ only, sequentially and simultaneously implanted tungsten. The C 1s XPS spectrum was found to be divided into two peaks; the lower peak located at 282.7 eV was attributed to C–W bond and the higher one at 284.6 eV was attributed to C–C bond. The peak areas for these peaks are summarized in Fig. 3. It is clear that the major chemical state for the C^+ only implanted tungsten is the C–C bond. However, in the case of sequentially implanted tungsten, the amount of C–C bond clearly decreased, indicating that the C–C bond was chemically sputtered by D_2^+ implantation. For the simultaneously implanted tungsten, not only C–W bond but also C–C bond existed. However, the amount of C–W bond was nearly constant among these three samples, C^+ only, sequentially and simultaneously implanted tungsten samples, indicating that the formation of C–W bond was saturated and the carbon with forming C–C bond was accumulated near the surface region of the tungsten sample.

Fig. 4 shows the D_2 TDS spectra for simultaneously implanted tungsten. The C^+/D^+ flux ratio was varied amongst these samples. In the case of $C^+/D^+ = 0.2$, the TDS spectrum was clearly different from the other spectra. The desorption stages were extended to higher temperatures, with the desorption shoulder appeared ∼800 K; similar to the desorption observed for sequentially implanted tungsten. For the $C^+/D^+ = 1$ case, the higher desorption stage at ∼800 K disappeared and only one large desorption peak was found at ∼350 K; similar to the desorption observed for the pure tungsten case. In the case of $C^+/D^+ = 2$, the desorption stage at 350 K disappeared and a large desorption peak was found at 500 K, corresponding to the desorption stage for deuterium retained in WC interstitial site. The deuterium retentions for the simultaneously implanted tungsten with various C^+/D^+ flux ratios are summarized in Fig. 5. The data for sequentially implanted tungsten with $C^+/D^+ = 1$ is also shown for comparison. It was clear that the highest deuterium retention was achieved for the sample with C^+/D^+ flux ratio of 0.2. The data was scattered as increasing the C^+/D^+ flux ratio. However, we believe that the deuterium retention would be converged by increasing the C^+/D^+ flux ratio above 1. Fig. 6 summarizes the peak area of C 1s XPS spectrum as a function of C^+/D^+ flux ratio. It was found that the carbon concentration decreased with increasing C^+/D^+ flux ratio, indicating the enhancement of carbon re-emission for high C^+/D^+ flux ratios.
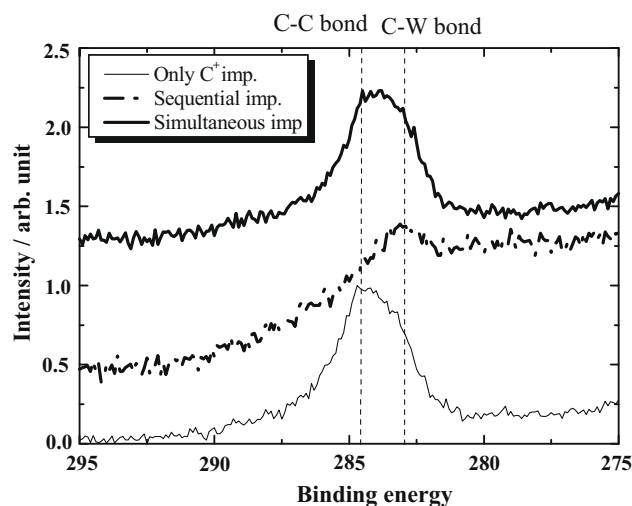

Fig. 1. The D_2 TDS spectra for sequentially and simultaneously implanted tungsten. Experimental results for pure tungsten and tungsten carbide are also shown.

Fig. 2. The C 1s XPS spectra for C^+ only, sequentially and simultaneously implanted tungsten. The C–W and C–C bonds were located at 282.7 eV and 284.6 eV, respectively.
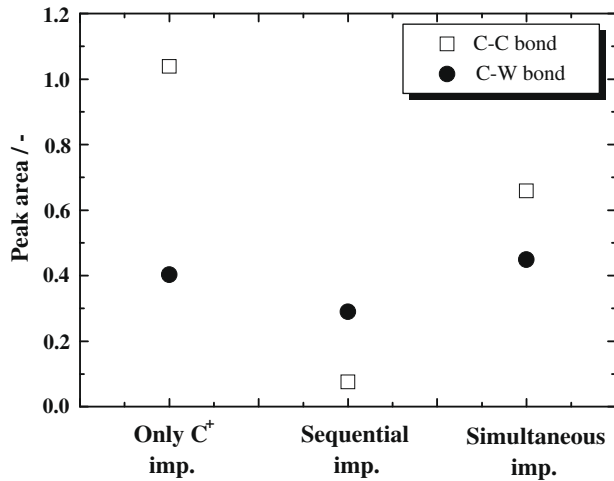
Fig. 3. The peak areas of C–W and C–C bonds for C+ only, sequentially and simultaneously implanted tungsten.
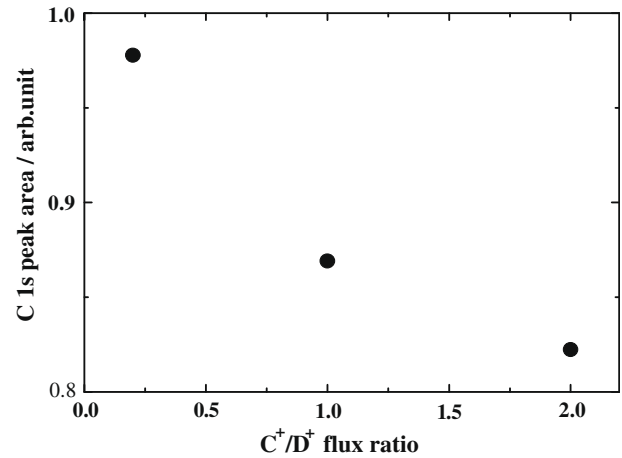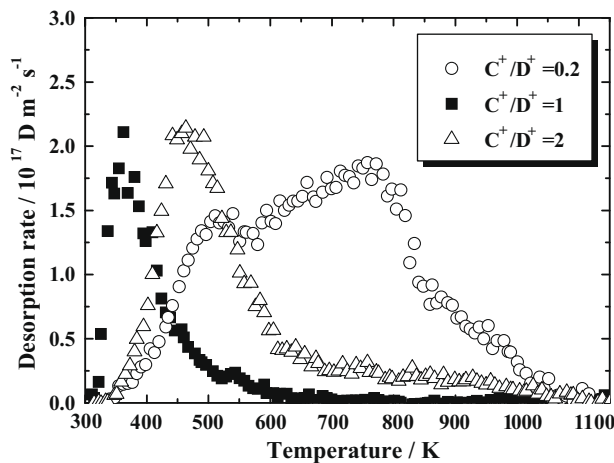

Fig. 4. The D_2 TDS spectra for the simultaneously implanted tungsten with varying C^+/D^+ flux ratio.
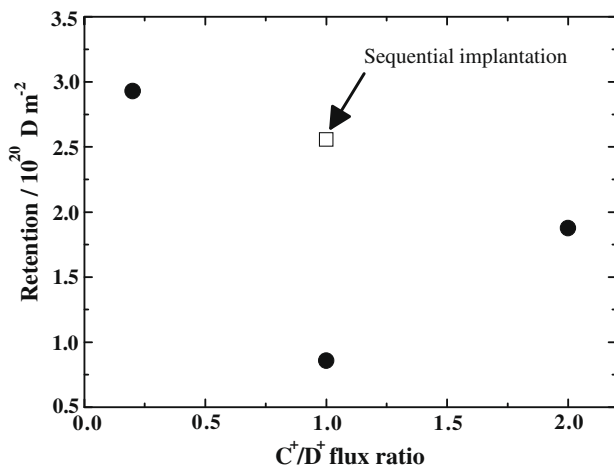
Fig. 5. Summary of deuterium retention for the simultaneously implanted tungsten with various C^+/D^+ flux ratio.

Fig. 6. Summary of C 1s peak areas as a function of C^+/D^+ flux ratio.

found in deuterium retention behavior between the sequential and simultaneous implantations. Large contribution on deuterium retention would be based on carbon retention. The amount of C–W bond in tungsten was almost uniform with all the samples, indicating that the number of C–W bonds would be limited. The residual carbon would form C–C bonds, which was easily sputtered by succeeding D_2^+ implantation in case of sequential implantation. Therefore some of deuterium would be bound to carbon forming C–D bonds in tungsten, which contribute to the higher temperature desorption stage of TDS. In the case of simultaneous implantation with the flux ration of $C^+/D^+ = 1$, the C–C bonds still remained in tungsten and simultaneous deuterium trapping with carbon in tungsten would not enhance deuterium retention, indicating that the sputtering by carbon would induce the dynamic deuterium desorption. Further study will be required to reveal more detailed mechanism. In addition, the C^+/D^+ flux ratio would be one key factor for deuterium retention in tungsten. In the low C^+/D^+ flux ratio, both of the deuterium retention evaluated by TDS and carbon concentration by XPS were the highest and they decreased as the C^+/D^+ flux ratio increased. In the C^+/D^+ flux ratio above 1, deuterium trapping by carbon was not found and it can be said that deuterium retention would be governed by the interstitial and available traps produced by ion implantation in tungsten. Therefore, the large amount of trapping sites would be produced for high C^+/D^+ flux ratio, which is quite consistent with the deuterium retention in tungsten in previous report, where the D retention is limited by the number of available traps [10]. However, in the low C^+/D^+ flux ratio, deuterium trapping by carbon would be one of major trapping states. This fact indicated that the sputtering cross-section by carbon would be low, and simultaneous carbon and deuterium trappings would be processed in tungsten. Our further studies will reveal the more detailed role of carbon on deuterium trapping in tungsten, especially at lower C^+/D^+ ratios.

4. Conclusion

To elucidate the C+ implantation effect on deuterium retention in tungsten, a simultaneous C+ and D_2^+ implantation experimental system was set up and sequential and simultaneous C+ and D_2^+ implantation experiments were performed on tungsten. It was found that deuterium retention for the simultaneous implanted tungsten with the flux ration of $C^+/D^+ = 1$ was lower than that for the sequential one, indicating that the sputtering by carbon would reduce deuterium trapping. In addition, deuterium retention decreased as the C^+/D^+ ion flux ratio increased and deuterium trap-

From these experimental results, C+ implantation effect on deuterium trapping in tungsten is discussed. A clear difference was

ping by carbon was not observed for high C^+/D^+ ratio. These facts indicated that the number of available traps in tungsten would mainly control the deuterium retention in tungsten. However, in the low C^+/D^+ ratio, deuterium trapping by carbon would be one of major trapping states, which would make high deuterium retention compared to pure tungsten.

Acknowledgement

References

[1] M. Kaufmann, R. Neu, Fus. Eng. Des. 82 (2007) 521.
[2] J. Pamela, G.F. Matthews, V. Philipps, R. Kamendje, J. Nucl. Mater. 363–365 (2007) 1.
[3] R.P. Doerner, J. Nucl. Mater. 363–365 (2007) 32.
[4] Ch. Linsmeier, J. Luthin, P. Goldstrab, J. Nucl. Mater. 290–293 (2001) 25.
[5] V. Kh. Alimov, Phys. Scr. T108 (2004) 46.
[6] O.V. Ogorodnikova, J. Roth, M. Mayer, J. Nucl. Mater. 313–316 (2003) 469.
[7] R.A. Anderl, R.J. Pawelko, S.T. Schuetz, J. Nucl. Mater. 290–293 (2001) 38.
[8] H. Kimura, Y. Nishikawa, T. Nakahata, M. Oyaidzu, Y. Oya, K. Okuno, Fus. Eng. Des. 81 (2006) 295.
[9] E. Igarashi, Y. Nishikawa, T. Nakahata, A. Yoshikawa, M. Oyaidzu, Y. Oya, K. Okuno, J. Nucl. Mater. 363–365 (2007) 910.
[10] I. Bizyukov, K. Krieger, N. Azarenkov, Ch. Linsmeier, S. Levchuk, J. Nucl. Mater. 363–365 (2007) 1184.
[11] J.F. Ziegler, SRIM Code, 2006, see <http://www.srim.org/>.